AMERICAN SOCIETY FOR MICROBIOLOGY | Microbiology Spectrum

RESEARCH ARTICLE

An Nuclear Magnetic Resonance Fingerprint Matching Approach for the Identification and Structural Re-Evaluation of *Pseudomonas* Lipopeptides

Vic De Roo,[a] Yentl Verleysen,[a,b] Benjámin Kovács,[a] Matthias De Vleeschouwer,[a,b] Penthip Muangkaew,[b] Léa Girard,[c] Monica Höfte,[d] René De Mot,[c] Annemieke Madder,[b] Niels Geudens,[a] José C. Martins[a]

[a]NMR and Structure Analysis Unit, Ghent University, Department of Organic and Macromolecular Chemistry, Ghent, Belgium
[b]Organic and Biomimetic Chemistry Research Group, Ghent University, Department of Organic and Macromolecular Chemistry, Ghent, Belgium
[c]Centre for Microbial and Plant Genetics, Faculty of Bioscience Engineering, KULeuven, Heverlee-Leuven, Belgium
[d]Laboratory of Phytopathology, Department of Plants and Crops, Faculty of Bioscience Engineering, Ghent, Belgium

Vic De Roo and Yentl Verleysen Contributed equally to this work. Author order was determined alphabetically.

ABSTRACT Cyclic lipopeptides (CLiPs) are secondary metabolites secreted by a range of bacterial phyla. CLiPs from *Pseudomonas* in particular, display diverse structural variations in terms of the number of amino acid residues, macrocycle size, amino acid identity, and stereochemistry (e.g., D- versus L-amino acids). Reports detailing the discovery of novel or already characterized CLiPs from new sources appear regularly in literature. Increasingly, however, the lack of detailed characterization threatens to cause considerable confusion, especially if configurational heterogeneity is present for one or more amino acids. Using *Pseudomonas* CLiPs from the Bananamide, Orfamide, and Xantholysin groups as test cases, we demonstrate and validate that the combined ^{1}H and ^{13}C Nuclear Magnetic Resonance (NMR) chemical shifts of CLiPs constitute a spectral fingerprint that is sufficiently sensitive to differentiate between possible diastereomers of a particular sequence even when they only differ in a single D/L configuration. Rapid screening, involving simple matching of the NMR fingerprint of a newly isolated CLiP with that of a reference CLiP of known stereochemistry, can then be applied to resolve dead-ends in configurational characterization and avoid the much more cumbersome chemical characterization protocols. Even when the stereochemistry of a particular reference CLiP remains to be established, its spectral fingerprint allows to quickly verify whether a newly isolated CLiP is novel or already present in the reference collection. We show NMR fingerprinting leads to a simple approach for early on dereplication which should become more effective as more fingerprints are collected. To benefit research involving CLiPs, we have made a publicly available data repository accompanied by a 'knowledge base' at https://www.rhizoclip.be, where we present an overview of published NMR fingerprint data of characterized CLiPs, together with literature data on the originally determined structures.

IMPORTANCE *Pseudomonas* CLiPs are ubiquitous specialized metabolites, impacting the producer's lifestyle and interactions with the (a)biotic environment. Consequently, they generate interest for agricultural and clinical applications. Establishing structure-activity relationships as a premise to their development is hindered because full structural characterization including stereochemical information requires labor-intensive analyses, without guarantee for success. Moreover, increasing use of superficial comparison with previously characterized CLiPs introduces or propagates erroneous attributions, clouding further scientific progress. We provide a generally applicable characterization methodology based on matching NMR spectral fingerprints of newly isolated CLiPs to natural and synthetic reference compounds with (un)known stereochemistry. In addition, NMR fingerprinting is shown to provide a suitable basis for structural dereplication. A publicly available

Editor Neha Garg, Georgia Institute of Technology

Address correspondence to José C. Martins, jose.martins@ugent.be, or Niels Geudens, niels.geudens@ugent.be.

The authors declare no conflict of interest.

Received 5 April 2022
Accepted 26 June 2022
Published 25 July 2022

reference compound repository promises to facilitate participation of the lipopeptide research community in structural assessment and dereplication of newly isolated CLiPs, which should also support further developments in genome mining for novel CLiPs.

KEYWORDS NMR spectroscopy, cyclic lipodepsipeptides, *Pseudomonas*, stereochemistry, dereplication

Pseudomonas represents a diverse and ubiquitous bacterial genus that evolves in a wide range of ecological niches (1, 2). To support their lifestyle and interactions with other organisms, they produce a variety of complex secondary metabolites including cyclic lipodepsipeptides or 'CLiPs' generated by non-ribosomal peptide synthetases (NRPSs) (3). Biological effects associated with these biosurfactant peptides include antimicrobial activity, control of bacterial motility, and biofilm formation and phytotoxicity, among others (4, 5). They are also involved in the complex interplay between bacteria and plants at the level of the plant rhizosphere. This generates plant growth promoting activity and protection against pathogens by direct antagonism or induced resistance (6, 7). Other reports have detailed anti-insecticidal activity (8, 9). As a result, this diverse array of functions of *Pseudomonas* CLiPs has sparked interest in their potential development in plant biocontrol applications and as biopesticides (10, 11). In turn, this also stimulates screening efforts for their development as novel antimicrobials (4, 5). Indeed, the current dearth of novel compounds to fight multidrug-resistant bacteria or fungal infections combined with an increased focus on the development of narrow-spectrum or even species-specific antibiotics has renewed efforts toward mining bacteria for novel pharmaceutical leads (12). These have included CLiPs, (13, 14) not in the least motivated by the successful introduction of daptomycin into clinical settings. In addition, several reports have highlighted anti-carcinogenic activities of *Pseudomonas* CLiPs, further illustrating their biomedical application potential (15–17). Therefore, both from a fundamental and application perspective, there is a pressing need to uncover the mode of action resulting in these biological functions, starting with the way these are related to the underlying chemical structures (5, 18, 19). Given that structure elucidation of CLiPs remains far from trivial, the development of reliable and straightforward approaches remains key. Moreover, such approaches should allow comparing different CLiPs to unequivocally establish their structural identity.

With well over 100 distinct chemical structures reported to date, *Pseudomonas* CLiPs invariably consist of an oligopeptide sequence of 8 to 25 residues, which is partly cyclized into a depsipeptide through ester bond formation of the C-terminus with a preceding side chain hydroxyl group (4, 5). An acyl chain of varying length and constitution caps the N-terminus of the oligopeptide sequence. The incorporation of non-proteinogenic amino acids, with a majority of residues displaying D-configuration through the action of epimerization domains in the non-ribosomal assembly line, generates additional structural diversity and further magnifies the structure elucidation challenge (20). The availability of rapid and affordable genome sequencing has stimulated the development of bioinformatic tools that allow to predict the CLiP structure produced by a particular non-ribosomal peptide synthetase (NRPS) by mapping its biosynthetic gene cluster (BGC) (21). The primary sequence is derived from analysis of the adenylation A-domains of the NRPS. Although separate epimerization domains are present in the siderophore synthetases of *Pseudomonas*, such activity is not found in their CLiP biosynthetic enzymes. Instead, condensation domains with intrinsic epimerization capacity (C/E) mimic the activity of a $^{D}C_{L}$ domain by converting the configuration of the C-terminal residue in the intermediate from L to D before extending the peptide (22). Tentative attribution of D/L configuration can therefore be inferred from analysis of the condensation domains involved. For *Pseudomonas* CLiPs in particular, the dual condensation/epimerization C/E domains responsible for configurational inversion of the preceding L-amino acid in the growing peptide chain can be identified using such tools, however it turns out that the epimerization functionality can be

inactive for reasons that remain unclear (23, 24). Consequently, as further demonstrated in this work, these predictions do not yet achieve the level of confidence necessary to eliminate the need for the more elaborate and labor-intensive chemical analysis methods. Furthermore, this genome-based approach does not provide information about the residues involved in the depsi bond, nor can the nature of the acyl chain be predicted. Thus, while analysis of the biosynthetic gene cluster coding for the NRPS represents a complementary asset during the chemical structure elucidation process (Fig. S1), it cannot replace it.

Combined application of mass spectrometric (MS) and NMR methods allows, in principle, to establish the composition of the oligopeptide sequence and the nature of the acyl chain as well as the cyclisation site but does not provide access to stereochemical information. For this, chemical derivatization methods combined with chromatographic separation, such as Marfey's analysis, are typically employed to derive the number and configuration of individual amino acids (Fig. S2) (25–28). However, the total hydrolysis of the lipopeptide into its constituent amino acids required in the process also causes the loss of information regarding their original position in the sequence. Consequently, positional ambiguity will arise when a particular amino acid with multiple occurrences in the sequence is configurationally heterogenous i.e., both the D- and L-configuration occur (26, 29). As a result, the elucidation of stereochemistry remains incomplete, such as is the case for the *Pseudomonas* CLiPs MDN-0066 (17), PPZPM-1a (30) and lokisin (31), among others. While workarounds exist, they are tedious and not error-proof (24, 26). In other cases, configurational analysis is omitted and configurational attribution is claimed by relying on either the conservation of the known pattern of D/L-configurations along a sequence (32, 33), or solely on genomic prediction (34–36). However, the latter ignores the problem of inactive epimerization domains (see above) while the former disregards the natural occurrence of diastereoisomeric lipopeptides having identical constitution but differing in configuration at one (or more) position(s). This is illustrated by, for example, the *Pseudomonas* CLiP pairs viscosin/WLIP, viscosinamide/pseudodesmin A, syringostatin/syringomycin and fengycin/plipastatin. Thus, new approaches that allow to move the structure elucidation beyond configurational dead-ends remain in high demand.

Simultaneously, the increased screening of *Pseudomonas* strains for CLiP production also calls for the introduction of dereplication approaches that confidently distinguish a known versus a novel CLiP structure early on, this to avoid the costly re-elucidation of previously described compounds (37). In line with this, multiple reports show a growing tendency to characterize known CLiPs from novel sources solely through comparison of their high resolution mass to those of previously characterized ones (32, 33, 38–43). However, these approaches overlook the possibility of isobaric lipopeptides, which occur more commonly than is perhaps anticipated. For instance, several members of the Viscosin group of CLiPs, such as viscosin and massetolide F, have a distinct molecular topology yet the same molecular formula, a situation that also occurs for milkisin and tensin, both members of the Amphisin group. Even lipopeptides from distinct CLiP groups can be isobaric, such as strikingly demonstrated by gacamide/cocoyamide and putisolvin II (44–46). Indeed, these share the same $C_{66}H_{115}N_{13}O_{19}$ molecular formula yet differ in the total number of amino acids (12 versus 11), the number of amino acids involved in the respective macrocycles (5 versus 4) and the constitution of the acyl chain (3R-OH C10:0 versus C6:0).

Previously, we noted that the combined ^{1}H and ^{13}C NMR chemical shift fingerprint obtained from ^{1}H-{^{13}C} HSQC spectra is sufficiently unique to differentiate diastereomers of a particular CLiP even when they differ in only a single D/L configuration (47). More so, it is sensitive to the configuration of the 3-hydroxy moiety of the fatty acid (HDA) tail as well (48). Indeed, inverting its configuration is also accompanied by changes in the ^{1}H and ^{13}C chemical shifts of the CH^{β} and CH^{α} resonances. By integrating NMR spectral fingerprinting and total synthesis into the existing bioinformatic and chemical analyses workflows commonly used for structure elucidation, we show here, for three representative cases, that configurational analysis dead-ends can be removed. First, by matching the ^{1}H-{^{13}C} HSQC spectral fingerprint of newly isolated *Pseudomonas* CLiPs with that of CLiPs of known

TABLE 1 Sequence, configurational analysis, and assignment of a novel Bananamide from *P. azadiae* SWRI103

Bananamide from SWRI103	AA1	AA2	AA3	AA4	AA5	AA6	AA7	AA8
Bioinformatic analysis workflow								
A-domain	Leu	Asp	Thr	Leu	Leu	Ser	Leu	Ile
C-domain	C_{start}	C/E	C/E	C/E	C/E	C/E	C/E	$^{L}C_{L}$
Prediction	D	D	D	D	D	D	L	L
Chemical analysis workflow								
NMR analysis	Leu	Glu	Thr	Leu	Leu	Ser	Leu	Ile
Marfey's analysis	L/D	D	D	L/D	L/D	D	L/D	L
Combined analysis and synthesized (8:6) Lx library								
	Leu	Glu	Thr	Leu	Leu	Ser	Leu	Ile
(8:6) L1 (1)[a]	**L**	D	D-a	D	D	D	L	L
(8:6) L4 (2)[a]	D	D	D-a	**L**	D	D	L	L
(8:6) L5 (3)[a]	D	D	D-a	D	**L**	D	L	L

[a]The nomenclature of the synthetic compounds is based on the (l:m) notation of the Bananamide group (8:7), followed by the position of the elusive L-Leu in the sequence (position 1, 4 or 5). Underlined amino acids are part of the macrocycle. The bold residues are those that differ from the predicted sequence.

stereochemistry obtained from total synthesis, we demonstrated the strength of our approach on the CLiP produced by *Pseudomonas azadiae* SWRI103^{T}. Next, the general applicability is shown by settling the stereochemistry of orfamide B from *Pseudomonas aestus* CMR5c and xantholysin A from *Pseudomonas mosselii* BW11M1, representative members from two other distinct *Pseudomonas* CLiP groups. In the process, we revise the stereochemistry of several orfamide homologues, including orfamide A from *Pseudomonas protegens* Pf-5, the original prototype CLiP defining the Orfamide group (49). Next, we proceed to illustrate how NMR fingerprinting constitutes a potent tool for CLiP dereplication purposes by resolving configurational dead-ends reported in literature for MDN-0066 (17), orfamides, and xantholysin produced by various bacterial strains, without the need for additional synthesis. Based on this, we advocate the adoption of NMR based fingerprinting by the CLiP research community and initiate establishing a data repository and knowledge database, which will be further developed toward this purpose.

RESULTS

Structure elucidation of a newly isolated Bananamide group member from *P. azadiae* SWRI103. (i) Isolation, bioinformatics, and initial chemical structure characterization. *P. azadiae* SWRI103 was originally collected from the rhizosphere of wheat in Iran, as part of a campaign to assess the plant growth stimulating potential of fluorescent pseudomonads (50). Initial PCR screening targeting initiation and termination domains indicated the presence of a lipopeptide-specific NRPS system (51). More recently, whole genome sequencing revealed a biosynthetic gene cluster (BGC) (52) with similarities to that of several Bananamide (8:6) producers, such as *Pseudomonas bananamidigenes* BW11P2 (37), *Pseudomonas botevensis* COW3 (53) and *Pseudomonas prosekii* LMG26867^{T} (54). Here, the (8:6) refers to the (l:m) notation we introduce to provide a simple but effective classification of CLiPs belonging to the same group from a chemical structure perspective, as explained in "Materials and Methods". As the stereochemistry of all these bananamides was unknown, we used strain SWRI103 to attempt full structure elucidation, which could only be achieved by the development of our expanded workflow, with all steps in the process described in detail hereafter (Fig. S1).

Firstly, analysis of the retrieved BGC predicted a Leu – Asp – Thr – Leu – Leu – Ser – Leu – Ile octapeptide sequence from the associated NRPS (Table 1). The total peptide sequence length and amphipathic profile matches that of previously reported and characterized bananamides (37, 53) but differs in amino acid composition. Therefore, it may represent a novel member of the Bananamide group (8:6). Next, bioinformatic analysis of the condensation/epimerization (C/E) domains was applied for the configurational analysis of the amino acids. The initial C_{start} domain is responsible for the

incorporation of a fatty acid (FA) moiety at the N-terminus of the peptide, the exact nature of which cannot be predicted. This domain is followed by six dual activity C/E domains, responsible for the condensation of the newly recruited L-amino acid to the growing peptide chain along with by L to D epimerization of the preceding residue in the sequence (55, 56). This is followed by one $^{L}C_{L}$-type domain, which lacks the epimerization functionality thus retaining the L-configuration of the preceding residue while incorporating an L-amino acid as final residue before cyclisation by a tandem of transesterification (TE) domains. Assuming that all dual C/E domains have functional epimerization activity, the combined A- and C-domain analysis predicts a FA – D-Leu – D-Asp – D-aThr – D-Leu – D-Leu – D-Ser – L-Leu – L-Ile sequence as the most likely lipopeptide biosynthesized by *P. azadiae* SWRI103 (Table 1).

Secondly, and independently from the bioinformatic analysis workflow, we engaged into the chemical analysis workflow of the putative novel bananamide. Following incubation of *P. azadiae* SWRI-103 in M9 minimal salt medium, a single CLiP-containing fraction could be extracted and purified. From high resolution MS analysis, a molecular mass of 1053.67 Da could be established i.e., within the expected range for an (8:6) CLiP. Next, NMR was used to elucidate the planar structure. That is, combined COSY/TOCSY analysis showed the presence of a single glutamic acid, serine, threonine, isoleucine, and four leucine residues in the peptide sequence while NOESY and ^{1}H-{^{13}C} HMBC experiments independently allowed to place these in the same order as predicted from the A-domain analysis, validating the latter (Table 1). Note however that while an aspartic acid residue was predicted at position 2 from the bioinformatic analysis, the presence of a glutamic acid was observed here using NMR spectroscopy. This is not surprising, as it was previously shown that Asp/Glu selectivity from genomic predictions is not always clear-cut (37). Additionally, the ^{1}H-{^{13}C} HMBC spectrum showed a clear $^{3}J_{CH}$ correlation between Thr3 H^{β} and Ile8 C′ thereby unambiguously establishing that the ester bond occurs between the hydroxyl side chain of threonine and the isoleucine carboxyl end, thus revealing the six-residue macrocycle expected for a member of the Bananamide group. Taking into account that $C_{52}H_{92}N_8O_{14}$ was derived as molecular formula from the HR-MS data, a 3-hydroxydecanoic moiety was inferred and confirmed from the NMR data while its linkage to the N-terminus resulted from characteristic $^{3}J_{CH}$ contacts with Leu1 in the ^{1}H-{^{13}C} HMBC spectrum. As neither MS nor NMR analysis allows establishing the configuration of the individual amino acid residues, we proceeded to Marfey's method for the analysis of amino acid configuration. Following total hydrolysis of the CLiP, Marfey's analysis allowed to unambiguously determine the configuration of all uniquely occurring residues. For the 6 leucines however, a 2:2 D:L ratio was found, indicating configurational heterogeneity and, as a result, the exact distribution of D and L-Leu residues within the oligopeptide sequence remained hidden. Therefore, at the end of the chemical analysis workflow, a total of 6 distinct sequences which all satisfy the 2:2 ratio but differ in the distribution of D- and L-leucines should therefore be considered. As a result, the definitive elucidation of the stereochemistry and, therefore, the chemical structure thus reaches a dead-end.

When information regarding a CLiP sequence is available from both bioinformatic and chemical analysis workflows, the configurational ambiguity is sometimes resolved by proposing that one of the sequences issued from chemical analysis matches the bioinformatic prediction (Fig. S1). However, such proposals should always be treated with caution since the epimerization functionality of C/E domains can be inactive in a currently unpredictable manner. Moreover, as aptly illustrated by all cases reported here, the predicted configuration from C-domain analysis may not even match those originating from the chemical analysis workflow. Here, for instance, the bioinformatic analysis proposes a 3:1 D:L ratio for the 4 leucines rather than the 2:2 found experimentally. Nevertheless, the bioinformatic analysis can still provide guidance to narrow down the number of possible diastereomeric sequences by noting that the $^{L}C_{L}$ domains, which lack the epimerization functionality, will maintain the L-configuration of the amino acid introduced at the preceding position (see above). Since such $^{L}C_{L}$ domain is present in the final NRPS module of *P. azadiae* SWRI103,

the penultimate Leu7 residue will invariably retain its L-configuration upon recruitment. This narrows down the number of possible sequences from 6 to 3: (8:6)-L1 (**1**), (8:6)-L4 (**2**) and (8:6)-L5 (**3**) (Table 1), depending on which leucine position features the remaining L-configuration. In all cases, the 3-hydroxy fatty acid tail is assumed to be (R)-configured, as is generally observed for *Pseudomonas* CLiPs. Notwithstanding the combination of bioinformatic and chemical analysis workflows, the stereochemistry remains ill-defined.

(ii) Extending the chemical analysis workflow by a synthesis add-on. As recently reviewed by Götze and Stallforth, several approaches exist to tackle the issue of configurational ambiguity (24). In the absence of suitable crystals for X-ray diffraction-based structure elucidation, the most common one resorts to mild acid catalyzed hydrolysis conditions or enzymatic degradation of linearized lipopeptides to yield oligopeptide fragments. These then need to be isolated, characterized by NMR or MS, and subjected to Marfey's method to identify the correct position of the corresponding D- or L-amino acids, introducing an extensive workload without guarantee that the matter will be settled (26). An alternative solution using MS makes clever use of deuterated amino acids and the fact that D-amino acids are, with very few exceptions, generated during biosynthesis through epimerization from L-amino acids (23, 57). In all cases, a separate analysis should be performed to elucidate the configuration of the 3-hydroxy fatty acid moiety (58). Here, we rather build on our previously developed total chemical synthesis route for Viscosin (9:7) group CLiPs (48, 59) to synthesize the 3 remaining (8:6)-Lx (x = 1, 4, 5) sequences (Table 1). The total chemical synthesis strategy mostly relies on solid phase peptide synthesis, affording considerable automation and rapid access to multiple homologous sequences through parallel synthesis (48, 59, 60). With one residue less in the macrocycle and a D-Glu2 rather than D-Gln2 as main differences, the synthesis of the (8:6)-Lx sequences could proceed with minimal change to the original strategy. A more extensive discussion of the applied synthesis route and its key features can be found in the Supplementary Materials section.

Next, the exact stereochemistry of the natural compound is revealed by matching the NMR spectral fingerprint to those of the synthetic compounds. The NMR matching approach relies on previous observations where, using the ^{1}H-{^{13}C} HSQC experiment, we established that the inversion in the configuration of a single Cα atom introduces prominent changes in the ^{1}H and ^{13}C chemical shifts of the corresponding (C–H)α group, even when the three-dimensional structure of the CLiP was retained (47). The same trend was found for the configuration of the 3-hydroxy fatty acid moiety (48). Thus, the (C–H)α fingerprint region of the HSQC spectra of the natural compound and its synthetic (8:6)-Lx analogue are expected to be identical. In contrast, the 2 other sequences will display clearly distinct HSQC spectra in general and (C–H)α fingerprint regions in particular as they feature 2 D:L inversions compared to the natural compound (Table 1).

By individually overlaying the ^{1}H-{^{13}C} HSQC spectra of each synthesized (8:6)-Lx variant with that of the natural compound from *P. azadiae* SWRI103, a straightforward visual assessment concerning similarities and differences in the ^{1}H and ^{13}C chemical shifts can be made (Fig. 1). Being the most sensitive reporters of backbone stereochemistry, we focus here on the cross-peaks in the (C-H)α fingerprint regions (Fig. 1). Accordingly, the (8:6)-L4 (2) variant shows an excellent match with the (C–H)α fingerprint of the natural compound since all (C-H)α cross peak pairs belonging to the same residue in the sequence show excellent overlap (Fig. 1A). In contrast, a considerable mismatch exists with (8:6)-L1 (1) as visualized by five clearly non-overlapping cross-peaks (Fig. 2B). This mismatch becomes even more pronounced for (8:6)-L5 (3), where essentially none of the cross-peaks overlap (Fig. 1C). Based on this, we can establish the stereochemistry of the *P. azadiae* SWRI103 bananamide as identical to that of the (8:6)-L4 (2) sequence (i.e., 3R-OH C10:0 – D-Leu – D-Glu – D-aThr – L-Leu – D-Leu – D-Ser – L-Leu – L-Ile), revealing that the C/E domain in the fifth module of the NRPS system is nonfunctional for epimerization. A more quantitative evaluation of spectral similarity is provided in the supplementary material section.

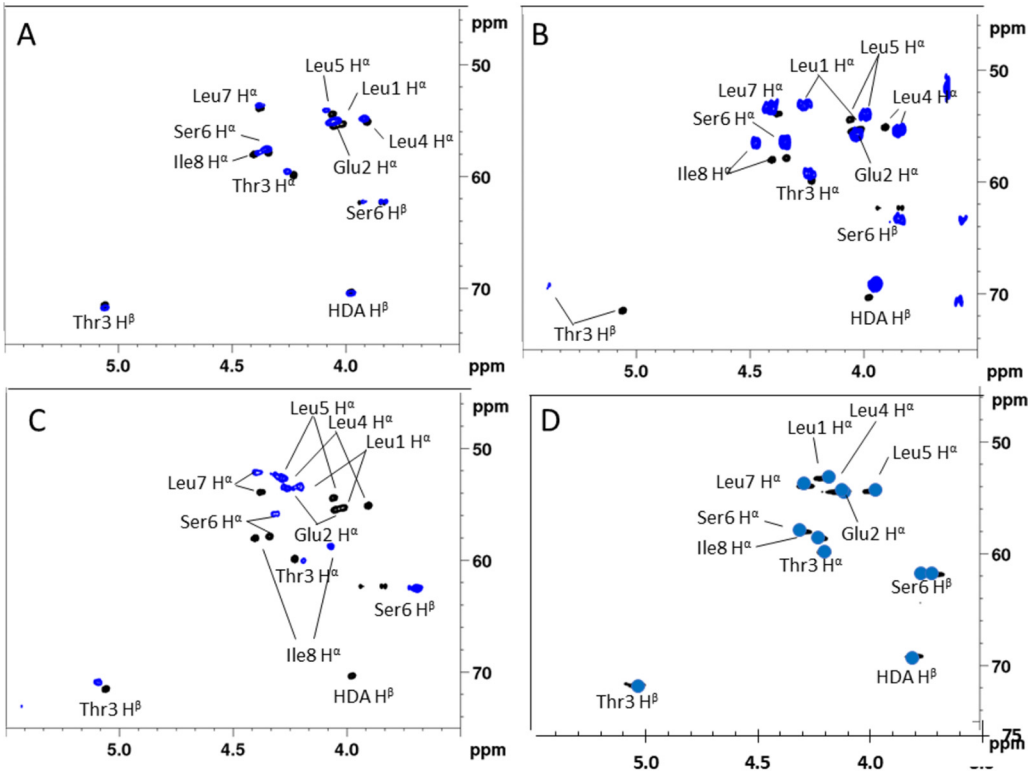

FIG 1 Comparison of the ^{1}H-{^{13}C} HSQC (CH)α fingerprints of the various synthetic (8:6)-Lx variants (blue) with that of the natural bananamide compound produced by *P. azadiae* SWRI103 (black) recorded in acetonitrile-d3 at 700 MHz, 303K. (A) Matching (8:6)- L4 variant (B) (8:6)- L1 variant and (C) (8:6)- L5 variant. (D) shows the spectrum of the natural compound but now recorded in DMSO-d6 at 298K (black) overlaid with a schematic representation of the spectrum of MDN-0066 which was recorded under identical conditions, generated from the tabulated chemical shift data in the original report (17).

In addition, to avoid any confusion regarding the absolute configuration of the 3-hydroxy decanoic acid, an analogue identical to L4 (2), but with a 3-(S)-hydroxydecanoic acid as fatty tail was synthetized as well (compound 2b). The overlay of this peptide with the natural compound revealed that inverting the configuration at this position clear affects the fingerprint region (supplementary information, S19). Indeed, the HSQC cross peak of the CH$^{\beta}$ of the fatty acid is shifted to the largest extent while additional shifts were also noticed at the level of the CH$^{\alpha}$ cross-peaks of Leu1, Glu2, and Thr3. This not only

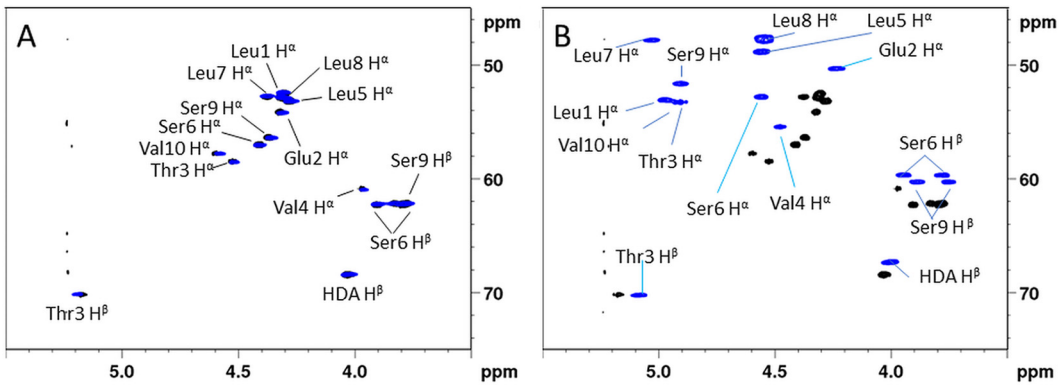

FIG 2 Comparison of the ^{1}H-{^{13}C} HSQC (CH)α fingerprint of synthetic (10:8)-Lx variants (blue) with that of the natural compound extracted from *P. aestus* CMR5c, all recorded in DMF-d7 at 500 MHz and 298K. (A) Overlay with the synthetic (10:8)-L1 variant (blue) and (B) the synthetic (10:8)-L5 variant (blue). A more quantitative evaluation of spectral similarity is provided in the supplementary material section.

confirms the possibility to discriminate the configuration at this position, but also the use of NMR based fingerprinting for configurational assignment.

(iii) Matching our reference compound with literature data. The effort to elucidate the stereochemistry of the *P. azadiae* SWRI103 (8:6) bananamide also allowed to settle that of MDN-0066, an (8:6) CLiP produced by *Pseudomonas granadensis* F-278,770^T, which showed distinct bioactivity in a renal carcinoma cell model (17). Using a chemical analysis methodology similar to the one described above, Cautain et al. (17) elucidated the peptide sequence by relying on MS analysis and NMR spectral assignment. However, the detailed stereochemical elucidation of MDN-0066 was left incomplete as Marfey's analysis revealed configurational heterogeneity given the presence of 2 D-Leu and 2x L-Leu, a result similar to that of the *P. azadiae* SWRI103 bananamide. Using the tabulated ^{1}H and ^{13}C NMR chemical shifts reported for MDN-0066 in DMSO-d6, the spectral fingerprint matching could be performed against the data of the SWRI103 bananamide recorded under identical conditions. The result, shown in Fig. 1D, shows a near identical match with (8:6)-L4 (2). This proves that MDN-0066 is identical to bananamide SWRI103, thereby disambiguating the stereochemistry of MDN-0066 and illustrating the potential of our approach for dereplication purposes. In order to assess the general applicability of our approach to *Pseudomonas* CLiPs, we then turned to 2 additional case studies, involving the stereochemical elucidation of orfamide B and xantholysin A.

Configuration elucidation of (10:8) orfamide B from *P. aestus* CMR5c. Orfamides are important for bacterial motility, cause lysis of oomycete zoospores, and play a role in biocontrol activity against fungal pathogens and insects (6, 49, 61–63). The name-sake of the Orfamide (10:8) group, orfamide A, was extracted from *Pseudomonas protegens* Pf-5 and fully characterized including its complete stereochemistry by mass spectrometry, NMR spectroscopy and chiral gas chromatography (49). Orfamides B and C were extracted as minors, and their planar structures were characterized as well. Since its original discovery, orfamide B is often found as the major compound produced by newly isolated bacterial strains (35). Additionally, the orfamide group has expanded with additional orfamide-homologues (30, 35, 64, 65). However, in many cases, the stereochemistry of orfamide B or that of other orfamide homologues from newly isolated bacterial sources remained unconfirmed as it was derived from sequence similarity with the original orfamide A as extracted from *P. protegens* Pf-5. To unlock conformational analysis and structure-activity evaluations for the Orfamide group, we therefore proceeded to an explicit stereochemical verification.

(i) Isolation, bioinformatics, and initial chemical structure characterization of orfamide B. *P. aestus* CMR5c was originally isolated from the rhizosphere of red cocoyam in Cameroon in a screen for biocontrol agents against the cocoyam root rot disease caused by *Pythium myriotylum* (11). We already reported the initial genome mining and bioinformatic analysis of the *P. aestus* CMR5c BGC which revealed the presence of 3 genes with ~80% similarity to the *ofaA*, *ofaB,* and *ofaC* NRPS genes from *P. protegens* Pf-5 (35). MS and NMR analysis further confirmed the predicted primary sequence and evidenced the incorporation of a 3-hydroxy-tetradecanoic acid moiety at the N-terminus. Thus, the major CLiP produced by *P. aestus* CMR5c has a planar structure identical to the originally published orfamide B. Based on this similarity in primary sequence and the genomic similarity between the respective BGCs, orfamide B from *P. aestus* CMR5c was proposed to also possess only L-leucines (35), as was previously also postulated for the original orfamide A (49).

C-domain analysis showed that the initial C_{start} type domain involved in acylating the first amino acid is followed by 6 dual activity C/E domains (modules 2–7), 2 non-epimerizing $^{L}C_{L}$ type domains (modules 8 and 9), and a final C/E domain in the last module (Table 2). Taking into account the distribution of $^{L}C_{L}$ and C/E domains, the bioinformatic analysis predicts the stereochemistry as shown in Table 2, with D-Leu residues occurring at positions 1 and 5 (Table 2) contradicting the all-L-Leu configuration proposed earlier. Marfey's analysis confirmed the configuration predictions for singly occurring amino acids and the 1:1 D:L ratio for both valines. For the leucines however, a

TABLE 2 Sequence, configurational analysis, and assignment of orfamide B from *P. aestus* CMR5c

CMR5c	AA[1]	AA[2]	AA[3]	AA[4]	AA[5]	AA[6]	AA[7]	AA[8]	AA[9]	AA[10]
Bioinformatic analysis workflow										
A-domain	Leu	Glu	aThr	Val/Ile	Leu	Ser	Leu	Leu	Ser	Val
C-domain	Cstart	C/E	C/E	C/E	C/E	C/E	C/E	$^{L}C_{L}$	$^{L}C_{L}$	C/E
Prediction	D	D	D	D	D	D	L	L	D	L
Proposal Ma et al. 2016 (33)	L	D	D	D	L	D	L	L	D	L
Chemical analysis workflow										
NMR analysis	Leu	Glu	Thr	Val	Leu	Ser	Leu	Leu	Ser	Val
Marfey's analysis	L/D	D	D-a	L/D	L/D	D	L/D	L/D	D	L/D
Synthesized Lx(10:8) library										
	Leu	Glu	Thr	Val	Leu	Ser	Leu	Leu	Ser	Val
(10:8)-L1 (4)[a]	L	D	D-a	D	**D**	D	L	L	D	L
(10:8)-L5 (5)[a]	**D**	D	D-a	D	L	D	L	L	D	L
(10:8) L1L5 (6)	L	D	D-a	D	L	D	L	L	D	L

[a]The nomenclature of the synthetic compounds is based on the (l:m) notation of the Orfamide group (10:8), followed by the position of the elusive L-Leu in the sequence (position 4, 5 or 4&5). The underlined residues in the tables indicate the position of the macrocycle. The bold residues are those that differ from the predicted sequence.

1:3 D:L ratio was found, invalidating the 2:2 ratio predicted from bioinformatic analysis as well as the all-L configuration proposed by Ma et al. (35).

(ii) Stereochemical elucidation using chemical synthesis and NMR fingerprint analysis. Considering the experimental evidence from the chemical analysis workflow, a total of 8 sequences should effectively be considered since the configurational D:L heterogeneity of the Leu and Val residues are combinatorically independent. Conveniently, the bioinformatic analysis allows to trim this down to 2 sequences only, strongly reducing the synthetic effort required. Indeed, the ambiguity regarding the valines can be settled by noting that, as the final residue, Val10 is not subjected to any epimerization activity. This pins the valine configurations down as D-Val4 end L-Val10. Next, the presence of $^{L}C_{L}$ domains in modules 8 and 9 allows to unequivocally attribute the L-configuration to Leu7 and L-Leu8. The remaining D and L configured leucines are to be distributed over positions 1 and 5. While this constitutes an apparent dead-end, configurational assignment could be finalized using fingerprint matching of the natural compound against the (10:8)-L1 (4**)** and (10:8)-L5 (5) sequences obtained by synthesis (Table 2) using the same strategy as discussed above for the bananamide analogues. This included the incorporation of a 3R-hydroxydecanoic moiety (3-OH C10:0) at the N-terminus rather than a 3R-hydroxytetradecanoic one (3-OH C14:0) mainly because of synthetic availability of the precursor. Previous investigation of C_{10}, C_{12} and C_{14} pseudodesmin analogues evidenced that lengthening of the acyl chain did not affect the ^{1}H and ^{13}C chemical shifts of the peptide moiety in any way (60).

Fig. 2 shows the overlay of the (C–H)α fingerprint region of each synthesized (10:8)-Lx sequence with that of natural orfamide B from *P. aestus* CMR5c. A straightforward visual assessment clearly indicates that the (10:8)-L1 (4) variant displays a near identical fingerprint match while none of the (C–H)α cross-peaks of (10:8)-L5 (5) overlap with those of the CMR5c orfamide. The latter probably indicates a major conformational effect caused by the L to D inversion at Leu5. To remove any doubts and independently exclude the all-L-Leu configuration originally proposed from sequence similarity with orfamide B from *P. protegens* Pf-5, we also committed to synthesize the corresponding (10:8)-L1L5 (6) analogue which again showed significant mismatch with the natural CMR5c orfamide. (Fig. S38) All data together establish that the stereochemistry of orfamide B from *P. aestus* CMR5c corresponds to that of the (10:8)-L5 (5) sequence (3R-OH C14:0 – L-Leu – D-Glu – D-aThr – D-Val – D-Leu – D-Ser – L-Leu – L-Leu – D-Ser – L-Val), indicating the C/E domain in the second module is non-functional for epimerization.

(iii) Stereochemical reassessment and dereplication of the Orfamide group using literature NMR data. The results presented above appear to indicate that orfamide B from *P. aestus* CMR5c is a D-Leu5 diastereoisomer of orfamide B from *P. protegens* Pf-5 (49), since the latter is reported to possess a L-Leu5. So far, reports of CLiPs from the

same (l:m) group that feature a configurational difference are few, possibly due to the lack of extensive configurational assignment among *Pseudomonas* CLiPs. The best-known example occurs within the Viscosin (9:7) group where CLiPs can be divided in a L-subgroup (14 sequences) and d-subgroup (5 sequences) depending on the configuration of the leucine, also at position 5 (66). Given that orfamides have been reported from multiple bacterial sources since their initial discovery, the question raised as to whether such division is also present for the Orfamide (10:8) group. Settling this matter would allow assessing whether stereochemical variation within a group is a more general feature present in the NRPS of *Pseudomonas* CLiPs. Conveniently, the major orfamides reported from other bacterial sources in literature feature planar structures identical to either orfamide A from *P. protegens* Pf-5 or orfamide B from *P. aestus* CMR5c, thus allowing the use of NMR fingerprinting for stereochemical evaluation. To be able to screen directly against a reference spectrum of orfamide A under standardized conditions, *P. protegens* Pf-5 was cultured to obtain orfamide A, together with a series of minor compounds including orfamide B and 4 previously unreported ones, which we named orfamides J – M (See supplementary information).

For the orfamide B producer *Pseudomonas sessilinigenes* CMR12a (67), the ^{1}H-{^{13}C} HSQC spectral fingerprint proved identical to the spectrum of the orfamide B reference from *P. aestus* CMR5c. This indicated that these molecules have identical stereochemistry and feature a D-Leu5. Next, we turn to *Pseudomonas* sp. PH1b where genome exploration revealed an orfamide-type BGC (68). Characterization of orfamides from this isolate presents an interesting case as it produces a major and a minor orfamide with sequence identical to orfamide A and orfamide B, respectively, thus only differing by a Ile4/Val4 substitution resulting from A-domain substrate flexibility in module 4 of the NRPS. The (C–H)α spectral fingerprint of its major orfamide matched with that of orfamide A produced by *P. protegens* Pf-5 indicating an L-configuration for Leu5. Surprisingly, however, the spectrum of the minor orfamide of *Pseudomonas* sp. PH1b matched with that of orfamide B from *P. aestus* CMR5c, therefore indicating a D-Leu5 configuration. This result was highly unexpected as it implies that in *Pseudomonas* sp. PH1b, the same NRPS assembly line would yield different configurations for Leu5. More specifically, it would require the occurrence of epimerization by the C/E domain of module 6 to correlate with the sequence composition of the growing peptide chain as recruited by module 4. Since the all-L Leu configuration of the original orfamide A from *P. protegens* Pf-5 was derived from extensive chemical analysis but not confirmed through total synthesis, it appeared more likely that an error was made in establishing the configuration at this position. To settle this matter, we reinvestigated the stereochemistry of the original orfamide A, as extracted from *P. protegens* Pf-5. In contradiction with the report by Gross et al., where chiral GC revealed a 0:4 D:L ratio for the leucines, our Marfey's analysis yielded a 1:3 D:L ratio, definitively settling the case in favor of a D-Leu5. As a result, in this case, configurational variability within one NRPS assembly line can be invalidated, and a revision is required for the configuration of Pf-5 based orfamides as shown in Table 2. Gratifyingly, this outcome was recently also arrived at using a completely independent approach involving total synthesis of orfamide A by Bando et al. (69), whereby the original stereochemistry led to loss of green algal deflagellation activity, while the corrected one was as active as the natural compound (70). Finally, we could establish that the orfamide produced by *Pseudomonas* sp. F6 (8) is identical to the revised orfamide A, by only making use of the tabulated chemical shift values of the published compound, and matching this to our reference spectrum of orfamide A (Fig. S43).

Settling the elusive stereochemistry of xantholysin A. An additional example illustrating the strength of our combined synthesis and spectral matching approach concerns xantholysin A. First reported as the main CLiP produced by *Pseudomonas mosselii* BW11M1, together with minor congeners B to D, it is the prototype that defines the Xantholysin (14:8) group (71). Since no configurational analysis was performed at the time, NMR and MS analysis only provided the planar structure. Subsequent reports proposed the production of xantholysins by other *Pseudomonas*

strains, uncovering a diverse portfolio of biological functions in the process. Pascual et al. (16) reported the production of xantholysins A to D by *Pseudomonas soli* F-279,208^T solely based on HR-MS of the isolates and characterized their cytotoxic activity against the RCC4 kidney carcinoma cell line. Lim et al. (9) reported HR-MS and ^{1}H NMR identical to those of xantholysin A and B for two lipopeptides from *Pseudomonas* sp. DJ15 and demonstrated their insecticidal activity against the green peach aphid, a major peach tree pest also serving as plant virus vector. In the context of exploring the tolerance of cocoyam plants against *Pythium myriotylum* in the field, Oni et al. (44) showed that *Pseudomonas* sp. COR51 produces a lipopeptide with identical planar structure to that of xantholysin A. It was also extracted and characterized from *Pseudomonas xantholysinigenes* in the framework of the development of a diagnostic bioinformatics tool that allows the assignment of a CLiP to a particular lipopeptide group based on the phylogeny of the *MacB* transporter of its producing bacterium. (54) In other work, a large-scale bacterial screening for antibiotic activity proposed the identification of xantholysins A-D in *Pseudomonas* sp. 250J, based on HR-MS data and high similarity in the NRPS genomic make-up to that of *P. mosselii* BW11M1 (72). Later on, combination of Marfey's analysis with mapping of the C/E and $^{L}C_{L}$ domains in its NRPS led to propose a stereochemistry for xantholysin A, although the distribution of the remaining D-Leu and L-Leu over positions 9 and 11 remained tentative (73). Shimura et al. (74) reported the total synthesis of MA026, a xantholysin-like CLiP from *Pseudomonas* sp. RtlB026 with potent anti-hepatitis C activity. Discrepancies in physicochemical properties of synthetic and natural MA026 led Uchiyama et al. (75) to revise its structure by exchanging residues at position 10 and 11, as previously suggested by Li et al. (71), thus leading to a planar structure identical to xantholysin A. With more than 90% sequence similarity between their respective BGC, it was proposed that the stereochemistry of xantholysin A would be identical to that of MA026. However, Uchiyama et al. (75) also noted that the stereochemical assignment for xantholysin A from *Pseudomonas* sp. 250J did not match with MA026, the latter containing L-Gln6 and D-Gln13, while the reverse configuration was proposed for the former.

To resolve this on-going characterization issue, we first considered applying our combined approach to the original xantholysin A from *P. mosselii* BW11M1. However, the presence of configurational heterogeneity for the leucine (D:L 2:1) and glutamine/glutamic acid (Glx) residues (D:L 4:1) independently act to generate 50 possible sequences, that can be trimmed down to 15 sequences when taking into account the genomic data. However, no further prioritization is possible after combining the chemical and genomic data. Comparison of the (C–H)α fingerprint of MA026 (with known stereochemistry) to that of originally isolated xantholysin A should in principle allow to either quickly establish configurational identity or eliminate one sequence. However, NMR data for MA026 was listed without explicit assignment. To circumvent this, we adapted our own synthesis scheme to produce MA026 and subsequently established that its (C–H)α fingerprint is indeed identical with that of the original xantholysin A (Fig. 3), thus avoiding the need for further synthesis. Used as reference compound, simple comparison of its (C–H)α fingerprint with that of putative xantholysin A lipopeptides allowed to also extend the assigned stereochemistry to the major xantholysin extracted from *Pseudomonas*. sp. COR51 (44), *P. xantholysinigenes* (54) and *Pseudomonas* sp. 250J (73), for which the NMR data were available or provided for comparison by the original authors, respectively. (Fig. S57, S58, and S59). In conclusion, the structure of xantholysin A was determined to be 3R-OH C10:0 – L-Leu – D-Glu – D-Gln – D-Val – D-Leu – L-Gln – D-Ser – D-Val – D-Leu – D-Gln – L-Leu – L-Leu – D-Gln – L-Ile. This reveals that two modules (2 in *XtlA* and 7 in *XltB*) lack the epimerization capability expected for the respective C/E-classified domains.

DISCUSSION

The discovery and development of new antimicrobial agents and therapies is an important avenue to tackle the rising global health threat caused by antimicrobial resistance (76, 77). Because of their broad range of antimicrobial activities and wide diversity

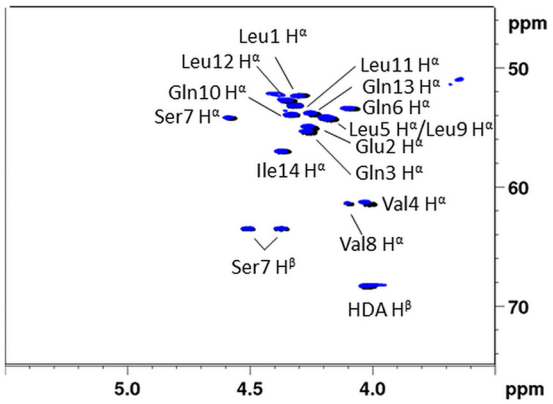

FIG 3 Comparison of the ^{1}H-{^{13}C} HSQC (C-H)α fingerprints of natural xantholysin A (14:8) produced by *P. mosselii* BW11M1 (black) with that of MA026 obtained through synthesis (blue). Both peptides were measured under identical conditions (DMF-d7, 328K, 700 MHz).

of structures, *Pseudomonas* CLiPs have drawn attention as an interesting class of compounds for further exploration in this respect (35, 60, 78, 79). To engage into structure-activity-relationship (SAR) studies, complete elucidation of their structure, including stereochemical make-up, is of vital importance to identify meaningful structure-activity associations (34, 59), and uncover their mode of action. Unfortunately, incomplete structure characterization increasingly accompanies the rising number of these CLiPs isolated from novel bacterial sources. Mass spectrometric (MS) data, genomic predictions or a combination thereof yield insufficient structural data by itself to generate a single structure elucidation result. Especially the comparative analysis with pre-existing data to establish structural novelty or identity with existing CLiPs is not approached critically enough to avoid erroneous attributions. Consequently, discovery efforts may generate a narrowed view on lipopeptide structural diversity due to erroneous assignment of *de facto* new structures to previously described ones. In turn, this clouds the comparative analysis and interpretation of antimicrobial activities of newly extracted compounds with already existing ones and threatens to lead subsequent development efforts astray. As natural product mining efforts aimed at *Pseudomonas* strains amplify, the chance of rediscovery of existing CLiPs increases as well. As a result, complete characterization including the labor-intensive determination of stereochemistry, while essential, may not provide a 'return-on- investment' as much effort might be spent on an already characterized compound (Fig. 4A).

As part of a concerted research effort aiming to map the structural and conformational diversity of *Pseudomonas* CLiPs, we extended the existing characterization workflows by a combined synthesis and NMR fingerprint matching approach. Simultaneously, it allowed us to demonstrate and validate the innate dereplication potential of the latter by a simple screening of the NMR fingerprint of newly isolated CLiPs. First, we established that the CLiP extracted from the newly isolated producer *P. azadiae* SWRI103 belongs to the Bananamide (8:6) group and subsequently resolved a configurational dead-end to reveal its stereochemistry. By utilizing our NMR spectral matching methodology, it was subsequently found to be identical to MDN-0066 produced by *the P. granadensis* type-strain, thereby settling the stereochemistry of this compound as well (17). Using the same approach, we determined that a structure revision is required for several, if not all, Orfamide (10:8) group members. While initially only poised to establish the stereochemical make-up of orfamide B as extracted from *P. aestus* CMR5c on a firmer basis, we showed that this compound possesses a D-Leu5, instead of an L-Leu5 as previously presumed and published (35, 49). Comparing the ^{1}H-{^{13}C} HSQC spectral fingerprint of a collection of CLiPs produced by *P. protegens* Pf-5, *P. sessilinigenes* CMR12a, *Pseudomonas* sp. F6, and *Pseudomonas*. sp. PH1b that share the orfamide sequence but have unreported stereochemistry, the presence of a D-Leu5 was confirmed in all cases, proving that one and the same compound is produced by diverse

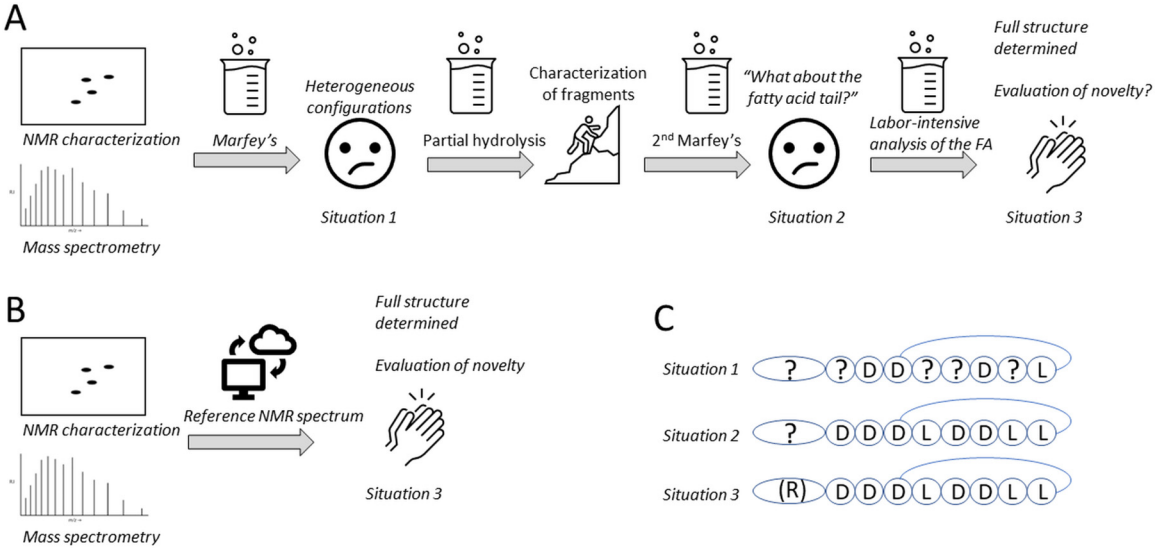

FIG 4 The stereochemical analysis of CLiPs requires a series of analysis steps. (A) Chemical analysis steps typically required before the implementation of our NMR fingerprint matching methodology described here. (B) Using NMR fingerprint matching, a single analysis step is required for identity confirmation as well as stereochemical validation. (C) Different levels of stereochemical validation of CLiPs.

strains from a variety of environments. Given an L-Leu5 was now confined to the originally reported orfamide A only, NMR fingerprint matching allowed to convincingly assert that here also, a D-Leu5 should be considered. Moreover, it was determined that all orfamide members possess a 3R-hydroxy-fatty acid tail, in contrast to earlier literature reports asserting the presence of a 3S-hydroxy-fatty acid tail (49, 58). Finally, we determined the stereochemistry of xantholysin A as produced by a variety of sources. Notably, with 15 possible sequences resulting from the combination of information obtained from both genomic as well as chemical analysis protocols, a considerable synthetic effort would have been required for the elucidation of this lipopeptides' stereochemistry. Instead, we utilized available literature data to prioritize possible sequences, resulting in only a single preferred sequence to be initially synthesized, thereby solving the stereochemistry of xantholysin A (as produced by various bacterial strains; using their reported literature data) and MA026.

From the above, it is clear that the NMR fingerprint approach introduced in this work has the potential to support researchers in dereplication, i.e., has this particular lipopeptide been isolated before? By matching NMR spectra of a CLiP from a newly isolated bacterial source with those of existing (reference) CLiPs, one can determine whether they are identical or not. Importantly, this is possible irrespective of the stereochemical characterization of the reference CLiPs and does not require any synthesis or extensive characterization effort. In fact, it can be performed at a relatively early stage following isolation and purification, as it only requires a ^{1}H-^{13}C fingerprint, which is preferably but not necessarily assigned. Indeed, in case of a perfect match, identity is ensured, while small but notable differences may motivate further characterization using the workflow as described here (Fig. S1).

It is important to note that total synthesis is not a prerequisite for dereplication of a newly isolated CLiP. In other words, the (C–H) α NMR fingerprint matching only requires the comparison of NMR spectra, or tabulated ^{1}H and ^{13}C chemical shifts values to assess structural similarity to a reference CLiP which may arise from natural sources or be synthetic compounds issued from structure elucidation efforts such as described in this work. Provided the required data is collected and made accessible, a fast screening method becomes available early on in the discovery process, potentially eliminating additional labor-intensive analyses, especially when it concerns CLiPs with a configurational heterogeneity of the amino acid content. Only when a genuinely new CLiP structure is found and/or no reference compound is available, additional analysis is desired/required. In such

cases, we have shown that genomic and chemical methods, in combination with solid-phase peptide synthesis can provide unambiguous characterization of CLiP structures.

Application of NMR based dereplication as introduced in principle here should permit an improved mining of NRPSs by providing reference data for bioinformatics software suites, thereby improving genomic prediction of CLiP structures. As previously observed for *Pseudomonas* lipopeptides from the Viscosin, Poaeamide, Tolaasin, Factin, Peptin, and Mycin families (29, 80) and further evidenced in this report for CLiPs from 3 additional groups (Bananamide, Orfamide, Xantholysin), the bioinformatic prediction of epimerization functionality in the non-ribosomal biosynthesis of CLiPs remains inaccurate. In each of these groups, at least 1 module appears catalytically inactive for epimerization. Only in the Amphisin (11:9) and Gacamide/Cocoyamide (11:5) groups do the predictions of dual activity condensation domains match with the elucidated CLiP stereochemistry. It can be anticipated that ensuring availability of unambiguous stereochemical information and scrutinizing corresponding C/E domain sequences for motifs linked to epimerization (in)activity (22), ideally complemented with insight from currently unavailable 3D structural C/E domain data, should allow an improved genomic prediction of the affected amino acid configurations.

Conclusion. Incomplete (or erroneous) structural characterization currently generates 'scientific noise' in the field of lipopeptide research, hampering a concerted research action for the generation of structure-activity relationships (18). The (C–H)α NMR fingerprint matching approach as described here will prevent this by offering a rapid, unambiguous characterization of CLiP structures. By standardizing the relevant experimental conditions as much as possible and by making reference data publicly available, a rapid elucidation of the complete structure of newly extracted lipopeptides, including stereochemical make-up of both the oligopeptide and the fatty acid moieties comes within reach (Fig. 4). In addition, our user friendly NMR matching methodology allowed to quickly supplement incomplete literature and characterization data with NMR fingerprint data, thereby elucidating the complete structure (including stereochemical make-up) of previously extracted CLiPs (Fig. S2). While limited to *Pseudomonas* CLiPs, our results support the (C–H)α NMR fingerprint matching as a tool for dereplication beyond this genus, such as those produced by other bacterial phyla, including *Bacillus*, *Burkholderia,* and *Streptomyces* spp. Indeed, without resorting to synthesis or elaborate chemical analysis, the identity of novel CLiPs from natural sources with previously, even only partially, characterized ones, can be established through matching of their spectra. Obviously, access to the desired NMR data for a sufficiently large collection of CLiPs, preferably with annotated fingerprints, is essential for this approach to become of use as dereplication tool for the research community. Only then can the lack of a match be interpreted as indicative of compound novelty with high confidence. While awaiting the development of a (dedicated) NMR data sharing and dereplication platform – most likely by integration of the reference spectra into existing (lipopeptide) databases, such as Norine (81, 82) – a publicly available NMR data repository accompanied by a 'knowledge base' has been made available at https://www.rhizoclip.be. It contains an overview of downloadable (C–H)α NMR fingerprint data of characterized CLiPs (both original spectra and tabulated chemical shift values), together with literature data on the originally determined structures. The latter includes a description of the CLiPs' original description, molecular mass, three-dimensional structures (if available), and a summary of published antimicrobial activities. Moreover, a detailed protocol is available for researchers that wish to record NMR data of their newly extracted lipopeptides to compare them to the publicly available reference data. Finally, we invite all researchers to submit NMR data of new CLiPs, such that they can be included in this knowledge base or contact us to explore possibilities to provide such data for their compounds.

MATERIALS AND METHODS

Detailed materials and experimental methods can be found in the SI appendix together with additional tables and figures.

Data availability. All study data are included in the article and *SI Appendix*. NMR data for (C–H)α spectral fingerprint matching can be found at https://www.rhizoclip.be.

SUPPLEMENTAL MATERIAL

Supplemental material is available online only.

SUPPLEMENTAL FILE 1, PDF file, 3.7 MB.

ACKNOWLEDGMENTS

A.M., M.H. and J.M. are recipients of a concerted research action grant (MEMCLiP) from Ghent University supporting this research (GOA-028-19). J.M., R.D.M., and M.H. are recipients of the Excellence of Science grant RhizoCLiP (EOS ID 30650620) supporting this research. The NMR equipment used in this work was funded through the FFEU-ZWAP initiative and grants from the Hercules Foundation (AUGE09/06 and AUGE15/12) awarded to a consortium headed by J. Martins. The NMR equipment is part of the NMR Centre of Expertise at UGent. We thank Pauline De Coster and Ilse Delaere for practical assistance with bacterial cultures, HPLC purifications, and NMR characterization. Thanks are extended to Kok-Gan Chan (University of Malaya, Malaysia) for use of the *Pseudomonas* sp. PH1B strain and Carlos Molina Santiago for providing the NMR spectral data of xantholysin A as extracted from *Pseudomonas* sp. 250J for fingerprint matching purposes.

J.C.M. designed the research with support from A.M., M.H., and R.D.M. N.G. managed the research effort. Y.V., V.D.R. and N.G. performed the majority of the research with assistance from B.K., P.M., M.D.V., and L.G. N.G. set up the Rhizoclip knowledge base with input from Y.V., V.D.R., and B.K. N.G. and J.C.M. wrote the original draft with all authors contributing toward scientific discussions and its finalization.

REFERENCES

1. Raaijmakers JM, De Bruijn I, Nybroe O, Ongena M. 2010. Natural functions of lipopeptides from *Bacillus* and *Pseudomonas*. FEMS Microbiol Rev 34:1037–1062. https://doi.org/10.1111/j.1574-6976.2010.00221.x.
2. Girard L, Lood C, Hofte M, Vandamme P, Rokni-Zadeh H, van Noort V, Lavigne R, De Mot R. 2021. The ever-expanding *Pseudomonas* genus: description of 43 new species and partition of the *Pseudomonas putida* group. Microorganisms 9:1766. https://doi.org/10.3390/microorganisms9081766.
3. Raaijmakers JM, Paulitz TC, Steinberg C, Alabouvette C, Moënne-Loccoz Y. 2009. The rhizosphere: a playground and battlefield for soilborne pathogens and beneficial microorganisms. Plant Soil 321:341–361. https://doi.org/10.1007/s11104-008-9568-6.
4. Geudens N, Martins JC. 2018. Cyclic lipodepsipeptides from *Pseudomonas* spp. – biological Swiss-army nnives. Front Microbiol 9:1867. https://doi.org/10.3389/fmicb.2018.01867.
5. Gotze S, Stallforth P. 2020. Structure, properties, and biological functions of nonribosomal lipopeptides from pseudomonads. Nat Prod Rep 37:29–54. https://doi.org/10.1039/c9np00022d.
6. Ma Z, Ongena M, Höfte M. 2017. The cyclic lipopeptide orfamide induces systemic resistance in rice to *Cochliobolus miyabeanus* but not to *Magnaporthe oryzae*. Plant Cell Rep 36:1731–1746. https://doi.org/10.1007/s00299-017-2187-z.
7. Prsic J, Ongena M. 2020. Elicitors of plant immunity triggered by beneficial bacteria. Front Plant Sci 11:594530. https://doi.org/10.3389/fpls.2020.594530.
8. Jang JY, Yang SY, Kim YC, Lee CW, Park MS, Kim JC, Kim IS. 2013. Identification of orfamide A as an insecticidal metabolite produced by *Pseudomonas protegens* F6. Agric Food Chem 61:6786–6791. https://doi.org/10.1021/jf401218w.
9. Lim DJ, Yang SY, Noh MY, Lee CW, Kim JC, Kim IS. 2017. Identification of lipopeptide xantholysins from *Pseudomonas* sp. DJ15 and their insecticidal activity against *Myzus persicae*. Entomological Res 47:337–343. https://doi.org/10.1111/1748-5967.12241.
10. Pedras MSC, Ismail N, Quail JW, Boyetchko SM. 2003. Structure, chemistry, and biological activity of pseudophomins A and B, new cyclic lipodepsipeptides isolated from the biocontrol bacterium *Pseudomonas fluorescens*. Phytochemistry 62:1105–1114. https://doi.org/10.1016/S0031-9422(02)00617-9.
11. Perneel M, Heyrman J, Adiobo A, De Maeyer K, Raaijmakers JM, De Vos P, Hofte M. 2007. Characterization of CMR5c and CMR12a, novel fluorescent *Pseudomonas* strains from the cocoyam rhizosphere with biocontrol activity. J Appl Microbiol 103:1007–1020. https://doi.org/10.1111/j.1365-2672.2007.03345.x.
12. Lewis K. 2013. Platforms for antibiotic discovery. Nat Rev Drug Discov 12:371–387. https://doi.org/10.1038/nrd3975.
13. Tracanna V, de Jong A, Medema MH, Kuipers OP. 2017. Mining prokaryotes for antimicrobial compounds: from diversity to function. FEMS Microbiol Rev 41:417–429. https://doi.org/10.1093/femsre/fux014.
14. Udaondo Z, Matilla MA. 2020. Mining for novel antibiotics in the age of antimicrobial resistance. Microb Biotechnol 13:1702–1704. https://doi.org/10.1111/1751-7915.13662.
15. Saini HS, Barragan-Huerta BE, Lebron-Paler A, Pemberton JE, Vazquez RR, Burns AM, Marron MT, Seliga CJ, Gunatilaka L, Maier RM. 2008. Efficient purification of the biosurfactant viscosin from *Pseudomonas libanesis* strain M9-3 and its physicochemical and biological properties. J Nat Prod 71:1011–1015. https://doi.org/10.1021/np800069u.
16. Pascual J, García-López M, Carmona C, Sousa T. d S, de Pedro N, Cautain B, Martín J, Vicente F, Reyes F, Bills GF, Genilloud O. 2014. *Pseudomonas soli* sp. *nov*., a novel producer of xantholysin congeners. Syst Appl Microbiol 37:412–416. https://doi.org/10.1016/j.syapm.2014.07.003.
17. Cautain B, de Pedro N, Schulz C, Pascual J, da SST, Martin J, Perez-Victoria I, Asensio F, Gonzalez I, Bills GF, Reyes F, Genilloud O, Vicente F. 2015. Identification of the lipodepsipeptide MDN-0066, a novel inhibitor of VHL/HIF pathway produced by a new *Pseudomonas* species. PLoS One 10:e0125221. https://doi.org/10.1371/journal.pone.0125221.
18. Geudens N, Sinnaeve D, Martins JC. 2018. Cyclic lipodepsipeptides: time for a concerted action to unlock their application potential? Future Med Chem 10:479–481. https://doi.org/10.4155/fmc-2017-0315.
19. Twigg MS, Baccile N, Banat IM, Deziel E, Marchant R, Roelants S, Van Bogaert INA. 2021. Microbial biosurfactant research: time to improve the rigour in the reporting of synthesis, functional characterization and process development. Microb Biotechnol 14:147–170. https://doi.org/10.1111/1751-7915.13704.
20. Roongsawang N, Hase K-i, Haruki M, Imanaka T, Morikawa M, Kanaya S. 2003. Cloning and characterization of the gene cluster encoding arthrofactin synthetase from *Pseudomonas* sp. MIS38. Chem Biol 10:869–880. https://doi.org/10.1016/j.chembiol.2003.09.004.

21. Medema MH, Fischbach MA. 2015. Computational approaches to natural product discovery. Nat Chem Biol 11:639–648. https://doi.org/10.1038/nchembio.1884.
22. Dekimpe S, Masschelein J. 2021. Beyond peptide bond formation: the versatile role of condensation domains in natural product biosynthesis. Nat Prod Rep 38:1910–1937. https://doi.org/10.1039/d0np00098a.
23. Scherlach K, Lackner G, Graupner K, Pidot S, Bretschneider T, Hertweck C. 2013. Biosynthesis and mass spectrometric imaging of tolaasin, the virulence factor of brown blotch mushroom disease. Chembiochem 14:2439–2443. https://doi.org/10.1002/cbic.201300553.
24. Gotze S, Stallforth P. 2020. Structure elucidation of bacterial nonribosomal lipopeptides. Org Biomol Chem 18:1710–1727. https://doi.org/10.1039/c9ob02539a.
25. Gerard J, Lloyd R, Barsby T, Haden P, Kelly MT, Andersen RJ. 1997. Massetolides A-H, antimycobacterial cyclic depsipeptides produced by two Pseumonads isolated from marine habitats. J Nat Prod 60:223–229. https://doi.org/10.1021/np9606456.
26. Gerhardt H, Sievers-Engler A, Jahanshah G, Pataj Z, Ianni F, Gross H, Lindner W, Lammerhofer M. 2016. Methods for the comprehensive structural elucidation of constitution and stereochemistry of lipopeptides. J Chromatogr A 1428:280–291. https://doi.org/10.1016/j.chroma.2015.05.065.
27. Fukuda TTH, Pereira CF, Melo WGP, Menegatti C, Andrade PHM, Groppo M, Lacava PT, Currie CR, Pupo MT. 2021. Insights into the ecological role of *Pseudomonas* spp. in an ant-plant symbiosis. Front Microbiol 12:621274. https://doi.org/10.3389/fmicb.2021.621274.
28. Bhushan R, Bruckner H. 2004. Marfey's reagent for chiral amino acid analysis: a review. Amino Acids 27:231–247. https://doi.org/10.1007/s00726-004-0118-0.
29. Götze S, Arp J, Lackner G, Zhang S, Kries H, Klapper M, Garcia-Altares M, Willing K, Günther M, Stallforth P. 2019. Structure elucidation of the syringafactin lipopeptides provides insight in the evolution of nonribosomal peptide synthetases. Chem Sci 10:10979–10990. https://doi.org/10.1039/C9SC03633D.
30. Weisshoff H, Hentschel S, Zaspel I, Jarling R, Krause E, Pham TLH. 2014. PPZPMs - a novel group of cyclic lipodepsipeptides produced by the *Phytophtora alni* associated strain *Pseudomonas* sp. JX090307 - the missing link between the viscosin and amphisin group. Natural Products Communications 9:989–996. https://doi.org/10.1177/1934578X1400900727.
31. Sorensen D, Nielsen TH, Sorensen J, Christophersen C. 2002. Cyclic lipoundecapeptide lokisin from *Pseudomonas* sp. strain DSS41. Tetrahedron Lett 43:4421–4423. https://doi.org/10.1016/S0040-4039(02)00856-0.
32. Loiseau C, Portier E, Corre MH, Schlusselhuber M, Depayras S, Berjeaud JM, Verdon J. 2018. Highlighting the potency of biosurfactants produced by *Pseudomonas* strains as anti-*Legionella* agents. Biomed Res Int 2018:8194368. https://doi.org/10.1155/2018/8194368.
33. Shahid I, Rizwan M, Mehnaz S. 2018. Identification and quantification of secondary metabolites by LC-MS from plant-associated *Pseudomonas aurantiaca* and *Pseudomonas chlororaphis*. Bio-Protocol 8:e2702. https://doi.org/10.21769/BioProtoc.2702.
34. Vallet-Gely I, Novikov A, Augusto L, Liehl P, Bolbach G, Pechy-Tarr M, Cosson P, Keel C, Caroff M, Lemaitre B. 2010. Association of hemolytic activity of *Pseudomonas entomophila*, a versatile soil bacterium, with cyclic lipopeptide production. Appl Environ Microbiol 76:910–921. https://doi.org/10.1128/AEM.02112-09.
35. Ma Z, Geudens N, Kieu NP, Sinnaeve D, Ongena M, Martins JC, Höfte M. 2016. Biosynthesis, chemical structure, and structure-activity relationship of orfamide lipopeptides produced by *Pseudomonas protegens* and related species. Front Microbiol 7. https://doi.org/10.3389/fmicb.2016.00382.
36. Gu Y, Ma Y-N, Wang J, Xia Z, Wei H-L. 2020. Genomic insights into a plant growth-promoting *Pseudomonas koreensis* strain with cyclic lipopeptide-mediated antifungal activity. MicrobiologyOpen 9:e1092. https://doi.org/10.1002/mbo3.1092.
37. Nguyen DD, Melnik A, Koyama N, Lu X, Schorn M, Fang J, Aguinaldo K, Lincecum TLJ, Ghequire MGK, Carrion VJ, Cheng TL, Duggan BM, Malone JG, Mauchline TH, Sanchez LM, Kilpatrick AM, Raaijmakers JM, De Mot R, Moore BS, Medema MH, Dorrestein PC. 2017. Indexing the *Pseudomonas* specialized metabolome enabled the discovery of poaeamide B and the bananamides. Nat Microbiol 2. https://doi.org/10.1038/nmicrobiol.2016.197.
38. Kissoyan KAB, Drechsler M, Stange E-L, Zimmermann J, Kaleta C, Bode HB, Dierking K. 2019. Natural *C. elegans* microbiota protects against infection via production of a cyclic lipopeptide of the viscosin group. Curr Biol 29:1030–1037. https://doi.org/10.1016/j.cub.2019.01.050.
39. Dagher F, Nickzad A, Zheng J, Hoffmann M, Deziel E. 2021. Characterization of the biocontrol activity of three bacterial isolates against the phytopathogen *Erwinia amylovora*. Microbiologyopen 10:e1202. https://doi.org/10.1002/mbo3.1202.
40. Oso S, Fuchs F, Übermuth C, Zander L, Daunaraviciute S, Remus DM, Stötzel I, Wüst M, Schreiber L, Remus-Emsermann MNP, Kivisaar M. 2021. Biosurfactants produced by phyllosphere-colonizing pseudomonads impact diesel degradation but not colonization of leaves of gnotobiotic *Arabidopsis thaliana*. Appl Environ Microbiol 87:e00091-21. https://doi.org/10.1128/AEM.00091-21.
41. Bernat P, Nesme J, Paraszkiewicz K, Schloter M, Płaza G. 2019. Characterization of extracellular biosurfactants expressed by a *Pseudomonas putida* strain isolated from the interior of healthy roots from *Sida hermaphrodita* grown in a heavy metal contaminated soil. Curr Microbiol 76:1320–1329. https://doi.org/10.1007/s00284-019-01757-x.
42. Zouari O, Lecouturier D, Rochex A, Chataigne G, Dhulster P, Jacques P, Ghribi D. 2019. Bio-emulsifying and biodegradation activities of syringafactin producing *Pseudomonas* spp. strains isolated from oil contaminated soils. Biodegradation 30:259–272. https://doi.org/10.1007/s10532-018-9861-x.
43. Ma Z. 2022. Analysis of the complete genome sequence of a rhizosphere-derived *Pseudomonas* sp. HN3-2 leads to the characterization of a cyclic lipopeptide-type antibiotic bananamide C. 3 Biotech 12:35. https://doi.org/10.1007/s13205-021-03100-3.
44. Oni FE, Geudens N, Omoboye OO, Bertier L, Hua HGK, Adiobo A, Sinnaeve D, Martins JC, Höfte M. 2019. Fluorescent *Pseudomonas* and cyclic lipopeptide diversity in the rhizosphere of cocoyam (*Xanthosoma sagittifolium*). Environ Microbiol 21:1019–1034. https://doi.org/10.1111/1462-2920.14520.
45. Jahanshah G, Yan Q, Gerhardt H, Pataj Z, Lammerhofer M, Pianet I, Josten M, Sahl HG, Silby MW, Loper JE, Gross H. 2019. Discovery of the cyclic lipopeptide gacamide A by genome mining and repair of the defective GacA regulator in *Pseudomonas fluorescens* Pf0-1. J Nat Prod 82:301–308. https://doi.org/10.1021/acs.jnatprod.8b00747.
46. Kuiper I, Lagendijk EL, Pickford R, Derrick JP, Lamers GEM, Thomas-Oates JE, Lugtenberg BJJ, Bloemberg GV. 2004. Characterization of two *Pseudomonas putida* lipopeptide biosurfactants, putisolvin I and II, which inhibit biofilm formation and break down existing biofilms. Mol Microbiol 51:97–113. https://doi.org/10.1046/j.1365-2958.2003.03751.x.
47. Geudens N, De Vleeschouwer M, Feher K, Rokni-Zadeh H, Ghequire MG, Madder A, De Mot R, Martins JC, Sinnaeve D. 2014. Impact of a stereocentre inversion in cyclic lipodepsipeptides from the viscosin group: a comparative study of the viscosinamide and pseudodesmin conformation and self-assembly. Chembiochem 15:2736–2746. https://doi.org/10.1002/cbic.201402389.
48. De Vleeschouwer M, Sinnaeve D, Van den Begin J, Coenye T, Martins JC, Madder A. 2014. Rapid total synthesis of cyclic lipodepsipeptides as a premise to investigate their self-assembly and biological activity. Chemistry 20:7766–7775. https://doi.org/10.1002/chem.201402066. 24817328.
49. Gross H, Stockwell VO, Henkels MD, Nowak-Thompson B, Loper JE, Gerwick WH. 2007. The genomisotopic approach: a systematic method to isolate products of orphan biosynthetic gene clusters. Chem Biol 14:53–63. https://doi.org/10.1016/j.chembiol.2006.11.007.
50. Rasouli Sedghiani MH, Khavazi K, Rahimian H, Malakouti MJ, Asadi Rahmani H. 2006. An evaluation of the potentials of indigenous fluorescent Pseudomonades of wheat rhizosphere for producing siderophore. Iranian J Soil and Water Sciences 20:133–142.
51. Rokni-Zadeh H, Mangas-Losada A, De Mot R. 2011. PCR detection of novel non-ribosomal peptide synthetase genes in lipopeptide-producing Pseudomonas. Microb Ecol 62:941–947. https://doi.org/10.1007/s00248-011-9885-9.
52. Zarvandi S, Bahrami T, Pauwels B, Asgharzadeh A, Hosseini-Mazinani M, Salari F, Girard L, De Mot R, Rokni-Zadeh H. 2020. Draft genome sequence of cyclic lipopeptide producer *Pseudomonas* sp. strain SWRI103, isolated from wheat rhizosphere. Microbiology Resources Announcement 9:e00538-20. https://doi.org/10.1128/MRA.00538-20.
53. Omoboye OO, Geudens N, Duban M, Chevalier M, Flahaut C, Martins JC, Leclere V, Oni FE, Hofte M. 2019. *Pseudomonas* sp. COW3 produces new Bananamide-type cyclic lipopeptides with antimicrobial activity against *Pythium myriotylum* and *Pyricularia oryzae*. Molecules 24:4170. https://doi.org/10.3390/molecules24224170.
54. Girard L, Geudens N, Pauwels B, Höfte M, Martins JC, De Mot R. 2021. Transporter gene-mediated typing for detection and genome mining of lipopeptide-producing *Pseudomonas*. Applied Environ Microbiol 88:e0186921. https://doi.org/10.1128/aem.01869-21.

55. Balibar CJ, Vaillancourt FH, Walsh CT. 2005. Generation of D amino acid residues in assembly of arthrofactin by dual condensation/epimerization domains. Chem Biol 12:1189–1200. https://doi.org/10.1016/j.chembiol.2005.08.010.
56. Roongsawang N, Lim SP, Washio K, Takano K, Kanaya S, Morikawa M. 2005. Phylogenetic analysis of condensation domains in the nonribosomal peptide synthetases. FEMS Microbiol Lett 252:143–151. https://doi.org/10.1016/j.femsle.2005.08.041.
57. Bode HB, Reimer D, Fuchs SW, Kirchner F, Dauth C, Kegler C, Lorenzen W, Brachmann AO, Grun P. 2012. Determination of the absolute configuration of peptide natural products by using stable isotope labeling and mass spectrometry. Chemistry 18:2342–2348. https://doi.org/10.1002/chem.201103479.
58. Karongo R, Jiao J, Gross H, Lammerhofer M. 2021. Direct enantioselective gradient reversed-phase ultra-high performance liquid chromatography tandem mass spectrometry method for 3-hydroxy alkanoic acids in lipopeptides on an immobilized 1.6 mum amylose-based chiral stationary phase. J Sep Sci 44:1875–1883. https://doi.org/10.1002/jssc.202100104.
59. De Vleeschouwer M, Martins JC, Madder A. 2016. First total synthesis of WLIP: on the importance of correct protecting group choice. J Pept Sci 22:149–155. https://doi.org/10.1002/psc.2852.
60. De Vleeschouwer M, Van Kersavond T, Verleysen Y, Sinnaeve D, Coenye T, Martins JC, Madder A. 2020. Identification of the molecular determinants involved in antimicrobial activity of pseudodesmin A, a cyclic lipopeptide from the viscosin group. Front Microbiol 11. https://doi.org/10.3389/fmicb.2020.00646.
61. Flury P, Vesga P, Pechy-Tarr M, Aellen N, Dennert F, Hofer N, Kupferschmied KP, Kupferschmied P, Metla Z, Ma Z, Siegfried S, de Weert S, Bloemberg G, Hofte M, Keel CJ, Maurhofer M. 2017. Antimicrobial and insecticidal: cyclic lipopeptides and hydrogen cyanide produced by plant-beneficial *Pseudomonas* strains CHA0, CMR12a, and PCL1391 contribute to insect killing. Front Microbiol 8:100. https://doi.org/10.3389/fmicb.2017.00100.
62. Ma Z, Hua GK, Ongena M, Hofte M. 2016. Role of phenazines and cyclic lipopeptides produced by *Pseudomonas* sp. CMR12a in induced systemic resistance on rice and bean. Environ Microbiol Rep 8:896–904. https://doi.org/10.1111/1758-2229.12454.
63. Olorunleke FE, Hua GK, Kieu NP, Ma Z, Hofte M. 2015. Interplay between orfamides, sessilins and phenazines in the control of Rhizoctonia diseases by *Pseudomonas* sp. CMR12a. Environ Microbiol Rep 7:774–781. https://doi.org/10.1111/1758-2229.12310.
64. Ma Z, Zhang S, Liang J, Sun K, Hu J. 2019. Isolation and characterization of a new cyclic lipopeptide orfamide H from *Pseudomonas protegens* CHA0. J Antibiotics 73:179–183. https://doi.org/10.1038/s41429-019-0254-0.
65. Zachow C, Jahanshah G, de Bruijn I, Song C, Ianni F, Pataj Z, Gerhardt H, Pianet I, Lammerhofer M, Berg G, Gross H, Raaijmakers JM. 2015. The novel lipopeptide poaeamide of the endophyte *Pseudomonas poae* RE*1-1-14 is involved in pathogen suppression and root colonization. Mol Plant Microbe Interact 28:800–810. https://doi.org/10.1094/MPMI-12-14-0406-R.
66. Geudens N, Nasir MN, Crowet JM, Raaijmakers JM, Feher K, Coenye T, Martins JC, Lins L, Sinnaeve D, Deleu M. 2017. Membrane interactions of natural cyclic lipodepsipeptides of the viscosin group. Biochim Biophys Acta Biomembr 1859:331–339. https://doi.org/10.1016/j.bbamem.2016.12.013.
67. D'Aes J, Kieu NP, Leclere V, Tokarski C, Olorunleke FE, De Maeyer K, Jacques P, Hofte M, Ongena M. 2014. To settle or to move? The interplay between two classes of cyclic lipopeptides in the biocontrol strain *Pseudomonas* CMR12a. Environ Microbiol 16:2282–2300. https://doi.org/10.1111/1462-2920.12462.
68. Chan X-Y, Hong K-W, Yin W-F, Chan K-G. 2016. Microbiome and biocatalytic bacteria in Monkey Cup (*Nepenthes pitcher*) digestive fluid. Sci Rep 6:20016. https://doi.org/10.1038/srep20016.
69. Bando Y, Hou Y, Seyfarth L, Probst J, Götze S, Bogacz M, Hellmich UA, Stallforth P, Mittag M, Arndt H-D. 2022. Total synthesis and structure correction of the cyclic lipodepsipeptide Orfamide A. Chemistry – A European Journal 28:e202104417. https://doi.org/10.1002/chem.202104417.
70. Hou Y, Bando Y, Flores DC, Hotter V, Schiweck B, Arndt H-D, Mittag M. 2021. Orfamide-A-mediated bacterial-algal interactions involve specific Ca^{2+} signalling pathways. bioRxiv. https://doi.org/10.1101/2021.07.24.453618.
71. Li W, Rokni-Zadeh H, De Vleeschouwer M, Ghequire MG, Sinnaeve D, Xie GL, Rozenski J, Madder A, Martins JC, De Mot R. 2013. The antimicrobial compound xantholysin defines a new group of *Pseudomonas* cyclic lipopeptides. PLoS One 8:e62946. https://doi.org/10.1371/journal.pone.0062946.
72. Molina-Santiago C, Udaondo Z, Ramos JL. 2015. Draft whole-genome sequence of the antibiotic-producing soil isolate *Pseudomonas* sp. strain 250J. Environ Microbiol Rep 7:288–292. https://doi.org/10.1111/1758-2229.12245.
73. Molina-Santiago C, Udaondo Z, Daddaoua A, Roca A, Martin J, Perez-Victoria I, Reyes F, Ramos JL. 2015. Efflux pump-deficient mutants as a platform to search for microbes that produce antibiotics. Microb Biotechnol 8:716–725. https://doi.org/10.1111/1751-7915.12295.
74. Shimura S, Ishima M, Nakajima S, Fujii T, Himeno N, Ikeda K, Izaguirre-Carbonell J, Murata H, Takeuchi T, Kamisuki S, Suzuki T, Kuramochi K, Watashi K, Kobayashi S, Sugawara F. 2013. Total synthesis and anti-hepatitis C virus activity of MA026. J Am Chem Soc 135:18949–18956. https://doi.org/10.1021/ja410145x.
75. Uchiyama C, Fukuda A, Mukaiyama M, Nakazawa Y, Kuramochi Y, Muguruma K, Arimoto M, Ninomiya A, Kako K, Katsuyama Y, Konno S, Taguchi A, Takayama K, Taniguchi A, Nagumo Y, Usui T, Hayashi Y. 2021. Structural revision of natural cyclic depsipeptide MA026 established by total synthesis and biosynthetic gene cluster analysis. Angew Chem Int Ed Engl 60:8792–8797. https://doi.org/10.1002/anie.202015193.
76. Murray CJ, Ikuta KS, Sharara F, Swetschinski L, Robles Aguilar G, Gray A, Han C, Bisignano C, Rao P, Wool E, Johnson SC, Browne AJ, Chipeta MG, Fell F, Hackett S, Haines-Woodhouse G, Kashef Hamadani BH, Kumaran EAP, McManigal B, Agarwal R, Akech S, Albertson S, Amuasi J, Andrews J, Aravkin A, Ashley E, Bailey F, Baker S, Basnyat B, Bekker A, Bender R, Bethou A, Bielicki J, Boonkasidecha S, Bukosia J, Carvalheiro C, Castañeda-Orjuela C, Chansamouth V, Chaurasia S, Chiurchiù S, Chowdhury F, Cook AJ, Cooper B, Cressey TR, Criollo-Mora E, Cunningham M, Darboe S, Day NPJ, De Luca M, Dokova K, et al. 2022. Global burden of bacterial antimicrobial resistance in 2019: a systematic analysis. Lancet 399:629–655. https://doi.org/10.1016/S0140-6736(21)02724-0.
77. Laxminarayan R, Duse A, Wattal C, Zaidi AKM, Wertheim HFL, Sumpradit N, Vlieghe E, Hara GL, Gould IM, Goossens H, Greko C, So AD, Bigdeli M, Tomson G, Woodhouse W, Ombaka E, Peralta AQ, Qamar FN, Mir F, Kariuki S, Bhutta ZA, Coates A, Bergstrom R, Wright GD, Brown ED, Cars O. 2013. Antibiotic resistance—the need for global solutions. Lancet Infect Dis 13:1057–1098. https://doi.org/10.1016/S1473-3099(13)70318-9.
78. Xue Y, Wang M, Zhao P, Quan C, Li X, Wang L, Gao W, Li J, Zu X, Fu D, Feng S, Li P. 2018. Gram-negative bacilli-derived peptide antibiotics developed since 2000. Biotechnol Lett 40:1271–1287. https://doi.org/10.1007/s10529-018-2589-1.
79. Rofeal M, El-Malek FA. 2021. Valorization of lipopeptides biosurfactants as anticancer agents. Int J Pept Res Ther 27:447–455. https://doi.org/10.1007/s10989-020-10105-8.
80. Girard L, Hofte M, Mot R. 2020. Lipopeptide families at the interface between pathogenic and beneficial Pseudomonas-plant interactions. Crit Rev Microbiol 46:397–419. https://doi.org/10.1080/1040841X.2020.1794790.
81. Caboche S, Pupin M, Leclère V, Fontaine A, Jacques P, Kucherov G. 2008. NORINE: a database of nonribosomal peptides. Nucleic Acids Res 36:D326–D331. https://doi.org/10.1093/nar/gkm792.
82. Pupin M, Esmaeel Q, Flissi A, Dufresne Y, Jacques P, Leclère V. 2016. NORINE: A powerful resource for novel nonribosomal peptide discovery. Synth Syst Biotechnol 1:89–94. https://doi.org/10.1016/j.synbio.2015.11.001.